



RESEARCH ARTICLE - ENGINEERING

Design a Dual Polarizations MIMO Antenna Based on Decoupling Elements for 5G Smart-Phones

Haider Saad ^{1*}, Mahmood F. Mosleh ¹, Raed Abd-Alhameed ²

¹Electrical Engineering Technical College, Middle Technical University, Baghdad, Iraq

²Faculty of Engineering and informatics, Bradford University, Bradford, UK

* Corresponding author E-mail: haidersaadct@mtu.edu.iq

Article Info.	Abstract
<p><i>Article history:</i></p> <p>Received 28 August 2022</p> <p>Accepted 15 October 2022</p> <p>Publishing 01 April 2023</p>	<p>This paper suggests a compact linear and circular polarization MIMO antenna for sub-6 GHz 5G smartphones. The proposed design can be divided into three parts: Firstly, a linear polarized dipole antenna is presented with dimensions of $1 \times 33.7 \times 32.5 \text{ mm}^3$ and exhibits an impedance bandwidth (IBW) of 3.24GHz ranging from 3.3GHz to 6.6GHz at $S_{11} < -10 \text{ dB}$. The second part includes a circular polarization CPW-Fed antenna with dimensions of $1 \times 23.2 \times 30 \text{ mm}^3$. The IBW of the CPW antenna is more than 4GHz, starting from 3.9GHz to more than 8GHz at an $S_{11} < -10 \text{ dB}$. The 3-dB axial ratio for the CP CPW antenna ranges from 4GHz to 7.38GHz. Finally, a combination of LP and CP antennas is presented to form a dual polarization MIMO system. A MIMO system consists of 5 elements; 4 elements are LP and 1 element is a CP antenna. The size of the MIMO system is $1 \times 82.5 \times 150 \text{ mm}^3$ printed on an FR-4 substrate. Two impedance bandwidths are found due to the use of two antenna types. The first one (S_{11}, S_{22}, S_{44}, S_{55}) equals 3.44GHz while the second (S_{33}) equals 4.33GHz. HFSS is used for designing and simulating the proposed structures, while CST is used for verifying the results.</p>
<p>This is an open-access article under the CC BY 4.0 license (http://creativecommons.org/licenses/by/4.0/)</p>	
<p>Publisher : Middle Technical University</p>	
<p>Keywords: Sub-6 GHz; 5G; LP; CP; CPW.</p>	

1. Introduction

Fifth-generation (5G) technology has been developed to enhance the network's data rate, energy efficiency, capacity, and dependability with a fast growth rate and a huge number of devices requiring wideband operating frequencies [1]. The band spectrum of the 5G network is divided into two frequency bands: Sub-6GHz and Millimeter wave (mm-waves). The first frequency band is around 3.5 GHz, which is also used in 4G Long Term Evolution (LTE) networks [2]. While the second frequency band is the millimeter wave that starts from 24 GHz, which was approved in 2016 by the Federal U.S. Communications Commission (FCC).

Due to this expansion in the wireless network, the need for antennas with reliable radiation and excellent characteristics that are compact in size, lightweight, and have a low profile is increased [3, 4]. Due to the characteristics of printed circuit antennas, including lightweight, simplicity of fabrication, low profile, and cheap cost, printed circuit antennas are commonly and frequently employed in wireless communication systems. Moreover, such antenna types can easily be embedded and integrated with device boards [5]. However, many types of conventional printed antennas may not satisfy such requirements as high-speed data rate, wideband; stable unidirectional radiation over a wideband of frequencies, and high gain [6-8].

Conventional Yagi antennas are employed frequently in wireless communication networks owing to their unidirectional radiating patterns and high gain [9]. Yagi antenna includes three parts; reflector, driver elements, and director [10]. Densmore and Huang suggested a planar microstrip Yagi antenna in 1991 as a combination of microstrip and Yagi antennas with the same Yagi antenna properties as high gain, cheap cost, steady radiation, and ease of manufacture and integration with circuit boards [11]. Many approaches are employed for developing and improving the performance of the planar Yagi structure. A Microstrip to Slotline feeding technique is proposed to achieve a wide impedance bandwidth, and the evaluated result is approximately 46% [12].

Next, the Microstrip antenna concept was first suggested by Deschamps in 1953. However, in the 1970s, both Howell and Munson developed practical antennas. The Microstrip Antenna's advantages, including; lightweight, low-profile, small-size, and easy to fabricate led to the use of such antennas for many wireless applications [13].

In 1990, the coplanar waveguide (CPW) Fed antennas were suggested. The CPW-Fed antenna is a printed circuit antenna type considered the most straightforward technique to achieve wide bandwidth [14-17]. Due to the narrow bandwidth with the microstrip antenna [18], researchers have worked to overcome the narrow bandwidth issue.

Nomenclature & Symbols			
4G	fourth generation	5G	fifth generation
LP	linear polarization	CP	circular polarization
FR-4	flame retardant	MIMO	multiple input multiple output
FCC	federal communications commission	CST	computer simulation technology
CPW	coplanar waveguide	HFSS	high-frequency structure simulator
EBG	electromagnetic bandgap	AR	axial ratio
ARBW	axial ratio bandwidth	S_{ij}	S-parameters

Many microstrip antenna configurations have been introduced to increase the antenna bandwidth by adding slots [19-23]. Moreover, it has been found that slot antennas based on coplanar waveguide (CPW) feedlines have a lot of advantages over microstrip antennas, such as broader bandwidth and lower dispersion and radiation loss [24].

The dual polarization antenna structure is frequently utilized in the mobile communication system to enhance the performance of the mobile communication system by utilizing polarization diversity (PD). Furthermore, dual polarization antennas are utilized for various communication purposes, such as satellite communication, due to the different uses and different applications of such structures [25].

A multi-input-multi-output (MIMO) antenna system has many advantages, such as the highest data rate, capacity, and the ability to minimize high fading in frequency and time-variant wireless channels [26]. In addition, the MIMO antenna has good radiation patterns with the required diversity, which may be analyzed using polarization, beam, and spatial diversity [27].

The mutual coupling problem is the main challenge in the MIMO antenna systems due to the separation distance between antenna elements. Many techniques are employed to mitigate the mutual coupling between the components of the MIMO system. The decoupling structures can be employed to mitigate the mutual coupling, such as a transmission line with a stub that leads to more signal paths between the elements [28]. Moreover, the Electromagnetic Bandgap structures (EBG) can be utilized to reduce the mutual coupling between the components of the MMO system [29]. Also, modifying the antenna structure's ground layer can be utilized to mitigate the mutual coupling between the MMO antenna components [30]. Furthermore, meta-surface walls between antenna elements can mitigate the mutual coupling by eliminating the surface waves [31].

This study suggests a MIMO antenna system with linear and circular polarizations for sub-6 GHz 5G smartphones. The overall size of the MIMO structure is $150 \times 82.5 \times 1 \text{ mm}^3$. The proposed MIMO system consists of 5 elements. 4 elements are placed on the corners of the rectangular substrate and give linear polarization. The other element is placed in the center of the substrate between two linearly polarized antennas and gives circular polarization. The fifth element is a CPW-Fed antenna, while the other four elements are planar dipole antennas. The proposed antennas have a good performance and bandwidth, encompassing the 5 G sub-6GHz applications. The Meander Line Resonator is added between MIMO elements to mitigate mutual coupling between them. The HFSS software is used for designing and simulating the suggested structures, while the CST is used for validating the results.

2. Related Works

Several studies use multiple techniques to design MIMO antenna systems. In [32], the authors present a 10 MIMO antenna system for smartphone applications. The proposed MIMO array total size is $140 \times 70 \text{ mm}^2$ printed on 0.8mm thick FR-4 dielectric substrate with a loss tangent of 0.02 and a relative permittivity equal to 4.4. Each antenna element in the MIMO structure is a type of microstrip line fed-open-slot antenna. The antenna array is operating at 3.6-GHz as a resonant frequency with a band starting from 3.4GHz to 3.8GHz for smartphone applications. In [33], the authors present a Dual Polarized 4×4 MIMO antenna structure for future wireless applications. The single microstrip antenna element size equals $55 \times 55 \text{ mm}^2$, while the overall MIMO structure dimensions are $165 \times 165 \text{ mm}^2$ printed on the FR-4 dielectric substrate of 1.6mm thick. MIMO antenna structure is found in operation at GSM (1.71GHz-1.88GHz), WLAN (5.15GHz-5.35GHz), and WiMAX (3.3GHz-3.7GHz) frequency bands. An axial ratio gives circular polarization bands equal to 94 MHz from (3.56-3.67) MHz for WiMAX and 203 MHz from (5.16-5.29) MHz for the WALN band. The GSM band gives linear polarization with an AR greater than 3 dB. In [34], investigates the design of three elements of MIMO antenna structure for linear and circular polarized Systems. Two antennas are used in the MIMO structure; a microstrip patch antenna and two printed dipole antennas. The MIMO antenna has a dimension of $29 \times 48 \text{ mm}^2$ and is printed on a 1.6mm dielectric substrate. The patch antenna is circularly polarized with a broadside radiation pattern while the printed dipole antenna has a linear polarized with end-fire radiation. The impedance bandwidth is found at 16.28 % at a resonant of 5.71 GHz for printed dipole, while it is found at 4.14 % at a resonant of 5.79 GHz for patch antenna. Finally, the 3dB axial ratio bandwidth is found from 5.61 to 5.70GHz.

In [35], the MIMO antenna design relies on Y-shaped antenna elements for Ultra-Wide Band applications. The MIMO antenna's total size is $150 \times 79 \text{ mm}^2$ printed on Rogers RO3003 dielectric substrate of thickness equal to 1.6mm and permittivity of 3. MIMO antenna system bandwidth is found to be 2.06 GHz, starting from 8.13GHz to 10.19GHz with a resonance frequency of 8.73GHz. Moreover, high isolation is achieved. In [36], the authors present a MIMO antenna structure for circularity and linearity polarization applications. The MIMO antenna size is $110 \times 47 \times 1.57 \text{ mm}^3$ printed on Rogers RT-droid 5880 substrate with a loss tangent of 0.0009 and a permittivity of 2.2. The MIMO antenna operates at a resonance frequency of 3.5GHz. In [37], designs an eight elements MIMO Antenna System for 5G future Mobiles. An inverted L-shaped monopole antenna element is used in the proposed design structure. The total size of the MIMO system is equal to $136 \times 68 \text{ mm}^2$ printed on an FR4 dielectric substrate that has 0.8mm thick. The proposed structure resonates at 3.5GHz (-6dB) with an IBW 450MHz. In [38], the authors present a MIMO antenna system for 5G sub-6GHz applications. The MIMO antenna system is characterized by a total size of $115 \times 65 \text{ mm}^2$ printed on an FR4 dielectric substrate of 1.6mm thickness. The operating bandwidth is found to be equal to 2.4GHz, from 3.6GHz to 5.8GHz, with a resonant frequency of 5.55GHz. The axial ratio (AR) is equal to 0.37 dB. In [39], the authors present a dual-polarized MIMO system for mobile applications. The total MIMO size is $150 \times 80 \times 1.6 \text{ mm}^3$ printed on an FR4 dielectric substrate. The MIMO antenna is resonating at 3.5GHz with an impedance bandwidth ranging from 3.4GHz to 3.6GHz.

3. Single-ELEMENT Linear Polarization Antenna

Fig. 1, shows the suggested antenna relying on the printed dipole antenna. The designed antenna is printed on an FR-4 dielectric substrate with a size of $32.5 \times 33.7 \text{ mm}^2$ ($L \times W$) and 1mm thick. The feedline employed for the suggested structure is a microstrip to slot-line transition with an impedance of 50ohm. The feed line is printed on the bottom face of the FR-4 dielectric substrate with a length of ($L_f = 18.3 \text{ mm}$). At the end of the transmission line, a square stub with dimensions of $4 \times 4 \text{ mm}^2$ ($S_1 \times S_2$) is inserted to increase impedance matching. The suggested antenna's patch layer is printed on the top surface of the dielectric substrate material. As shown in Fig. 1, the construction of the patch layer includes a reflector, flare-shaped drivers, and a single director. The driver is featured by having a flared shape and a tapered slotted curve. The length of each wing (L_3) is 8.4mm and the width (W_3) is 12mm. This curve is employed in the suggested structure because it has many advantages, such as wide IBW, symmetrical radiation pattern, and high gain. Adding the director to the antenna structure enhances the antenna's performance. The director has a size of $12 \times 1.5 \text{ mm}^2$ ($L_d \times W_d$). The antenna is featured by its given end-fire radiation pattern. Finally, the geometrical information of the suggested antenna is given in Table 1.

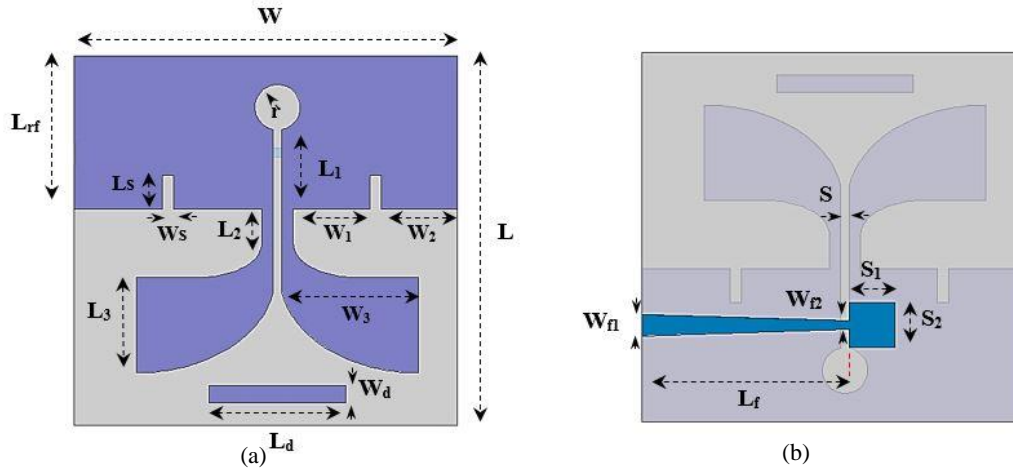


Fig. 1. Geometry of the linearly polarized dipole antenna (a) top view, and (b) bottom view

Table 1. The Parameter values of the linearly polarized dipole antenna

Parameter	Value (mm)	Parameter	Value (mm)
W_s	1	L_f	18.3
W_2	6.7	S_2	4
W_1	6.7	S_1	4
W	33.7	W_3	12
R	1	W_d	1.5
L_s	3	W_{f2}	0.8
L_{rf}	13.5	L_d	12
L_2	3	S	0.8
L_1	7	W_{f1}	1.9
L	32.5	L_3	8.4

4. Single-Element Circular Polarization Antenna

The suggested antenna structure relies on the CPW-Fed antenna and is depicted in Fig. 2. The proposed antenna structure is printed on a cheap FR-4 substrate. The dimension of the printed antenna is $30 \times 23.2 \text{ mm}^2$ ($L \times W$) with a 1mm substrate thickness. The feedline used in the suggested design is the coplanar waveguide (CPW), and it is printed on the top face of the dielectric substrate and has an impedance of 50ohm. The CPW waveguide consists of three parts: a stripline and two ground planes. Asymmetrical ground planes are used in the proposed antenna to give more IBW and more axial ratio bandwidth (ARBW). The gap between the feedline and the ground planes is evaluated and optimized, equaling 0.3mm.

The antenna is characterized by a single layer printed on one face of the substrate. As depicted in Fig. 2, the suggested antenna includes a radiating structure and asymmetrical rectangular grounds with a Corner Truncated Square Aperture. The radiating structure of the suggested antenna is characterized by a square shape with a size of $7.5 \times 8 \text{ mm}^2$ ($L_p \times W_p$), while the full ground planes are characterized by a size of $30 \times 23.2 \text{ mm}^2$. The other geometrical details of the proposed CPW-Fed printed antenna are presented in Table 2.

The radiator of the antenna and the feedline are shifted to the right side of the ground layer as seen in Fig. 2. This shift is helpful to improve the antenna's performance and the axial ratio. The right ground plane is featured by a size of $6 \times 6.725 \text{ mm}^2$ ($L_{G1} \times W_{G1}$), while the left ground plane is featured by a size of $9 \times 13.45 \text{ mm}^2$ ($L_{G2} \times W_{G2}$). The length of the CPW-Fed is 9.5mm while the width (W_f) is 2.5 mm.

As seen in Fig. 2, a straight line is used to improve the antenna performance where it surrounds the radiator of the antenna and is connected to the left ground only, while an open slot is on the right. The opened slot is useful to generate circular polarization by providing a perturbation with current distribution. Also, adding an inverted strip with a tangent line/triangular in both the upper right corner and lower left-corner of the proposed antenna slotted ground can enhance the ARBW by providing perturbation for the current distribution.

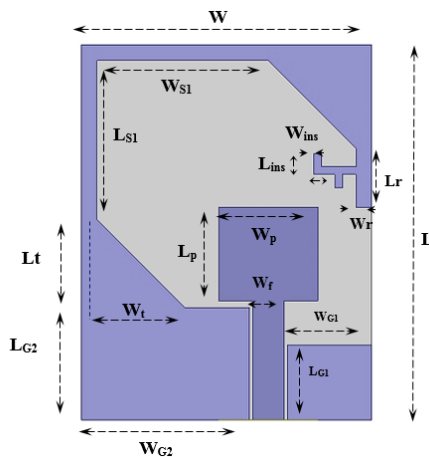


Fig. 2. The geometry of the circular polarization CPW-Fed printed antenna

Table 2. The Parameter values of the circular polarization CPW-Fed antenna

Parameter	Value (mm)	Parameter	Value (mm)
W_t	7	W_p	8
W_{S1}	13.775	L_{S1}	12.75
W_{G2}	13.45	W_r	1.25
W_{G1}	6.725	W_{ins}	0.625
W	23.275	W_f	2.5
L_t	7	L_p	7.5
L_{G2}	9	L_r	4.75
L_{G1}	6	L_{ins}	1.687
L	30		

5. MIMO Antenna System

After finishing the design process for both linear and circular polarization proposed antennas, and the optimum design is achieved, a combination between both antennas is made as a MIMO antenna system to achieve both polarization types in one structure, as depicted in Fig. 3. The optimal design includes five antenna element structures. The suggested optimal MIMO antenna construction is printed on a dielectric FR-4 material that has $\tan\delta = 0.02$ and $\epsilon_r = 4.4$. The overall size of the MIMO antenna structure is $150 \times 82 \text{ mm}^2$ ($L_m \times W_m$) with a thickness of 1mm for the substrate material. Due to the characteristics and properties of both the antenna types, the planar dipole antenna, and the CPW-Fed printed antenna, that is used in the MIMO structure, the five elements are arranged in some way to produce an omni-directional radiating pattern. The planner dipole antenna that has end-fire radiation is placed in the corners of the FR4 substrate each one is directed toward one of the four directions, while the CPW-Fed printed antenna of the quise omni-directional radiation pattern is placed in the center of the substrate so that the omni-directional radiation pattern will be achieved. This configuration is utilized to cover the whole four directions and obtain omni-directional-radiation. The geometrical information of the MIMO system is given in Table 3. In Fig. 4, A Meander Line Resonator technique between the antennas of the MIMO structure is presented with a size of $33.73 \times 9 \text{ mm}^2$ ($L_M \times W_M$). Such resonator technique is used and added between the MIMO components to mitigate the mutual coupling between the antennas and achieve good isolation. The geometrical details of the resonator are presented in Table 3.

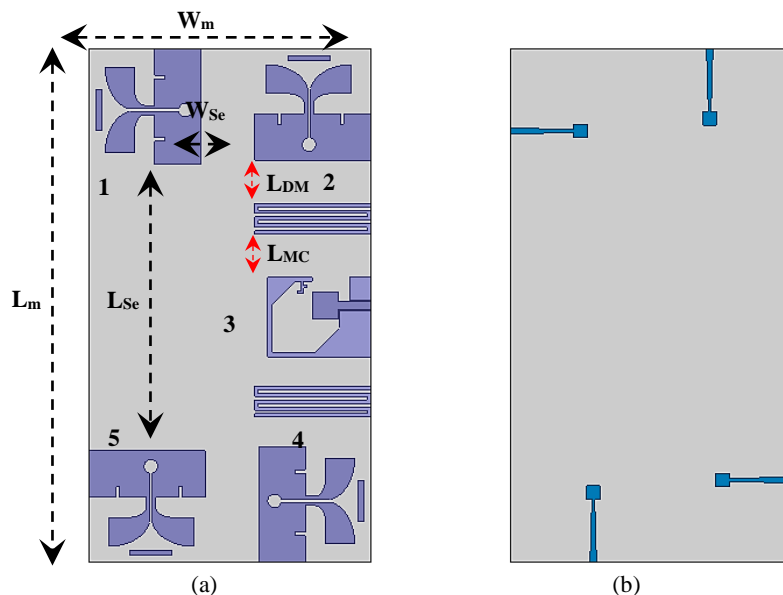


Fig. 3. The geometry of the dual polarization MIMO system (a) top layer and (b) bottom layer

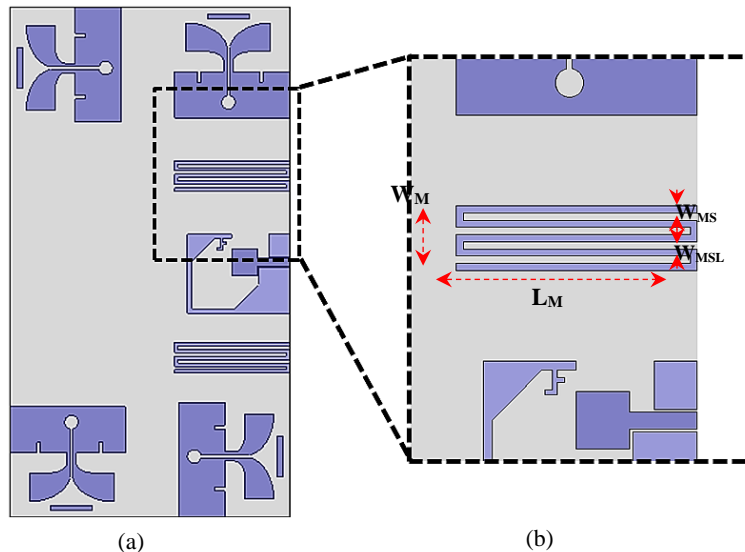


Fig. 4. (a) MIMO Antenna structure based on decoupling elements, and (b) Decoupling element (Meander line resonator)

Table 3. The Parameter values of the dual polarization MIMO system

Parameter	Value (mm)	Parameter	Value (mm)
L_m	150	L_{MC}	12.612
W_m	82	L_M	33.737
L_{Se}	83.7	W_M	9
W_{Se}	15.7	W_{MS}	1
L_{DM}	12.612	W_{MSL}	1

6. Results and Discussion

After finishing the design process of the suggested antenna structures, the proposed antennas are simulated and analyzed by the use of the HFSS software. The results of all proposed antennas will be expressed in terms of reflection coefficient (sii), gain, axial ratio, and radiation pattern.

6.1. Linear Polarization Antenna

Fig. 5 shows the evaluation of the linearly polarized antenna's reflection coefficient (S_{11}). Fig. 5 found that the simulated results show an IBW equal to 3.24GHz ranging from 3.3GHz to 6.6GHz at (-10 dB) which covers the whole 5G sub-6GHz band applications.

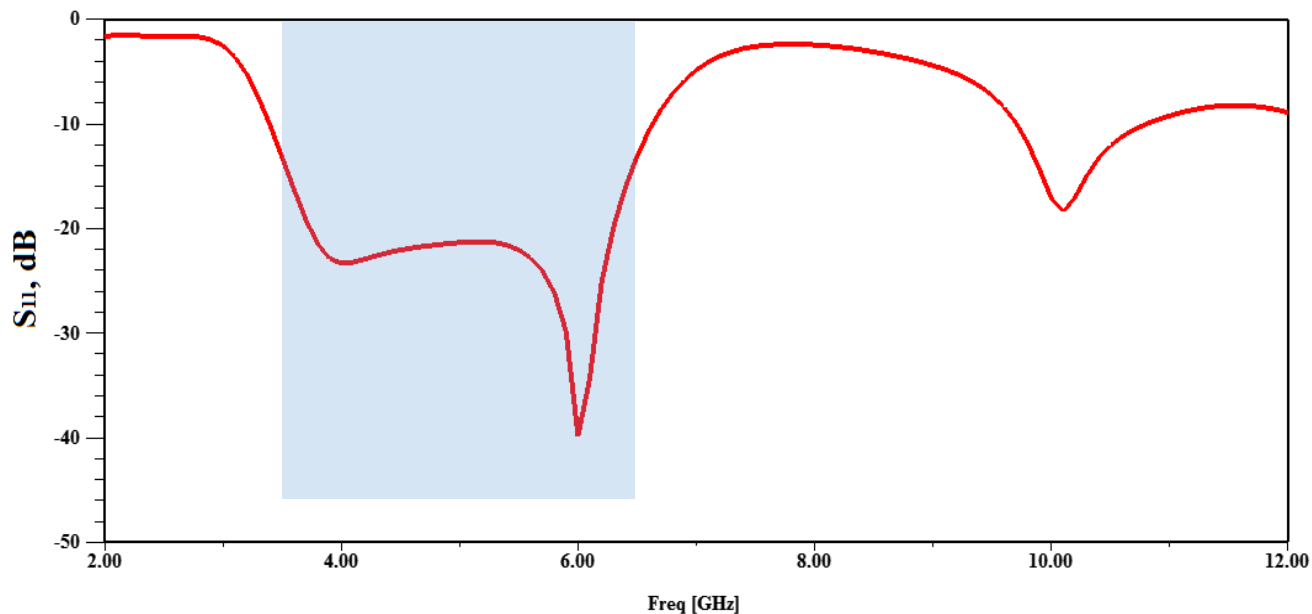


Fig. 5. The reflection coefficient (S_{11}) in dB for the LP printed dipole antenna

In Fig. 6, the gain for a linearly polarized printed antenna is displayed. As seen in Fig. 6, the gain varies from 5.2dB to 7.05dB in the whole operational frequency band.

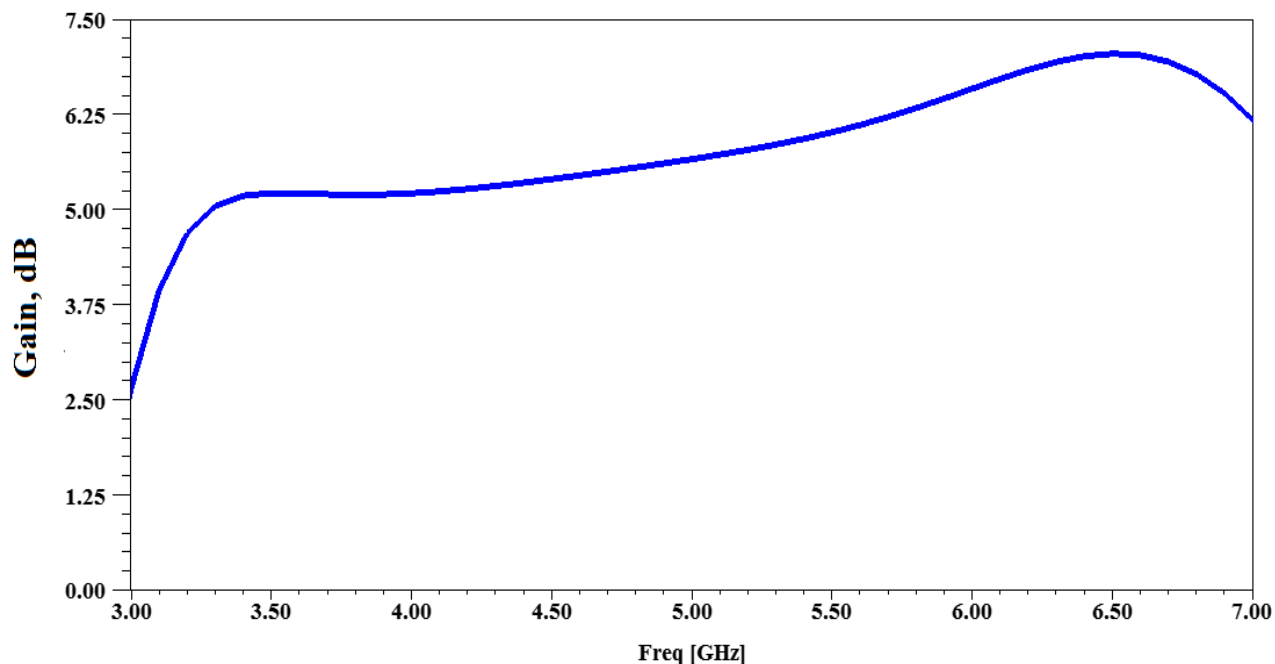


Fig. 6. The gain in dB for the LP printed dipole antenna

Next, the axial ratio is evaluated and presented in Fig. 7. The AR is a significant parameter to determine whether the antenna has linear or circular polarization. When the AR is smaller than 3dB then the antenna has circular polarization otherwise the antenna has linear polarization according to [40]. As depicted in Fig. 7, the antenna shows a linear polarization where the value of the AR is more than 3 dB in the whole band.

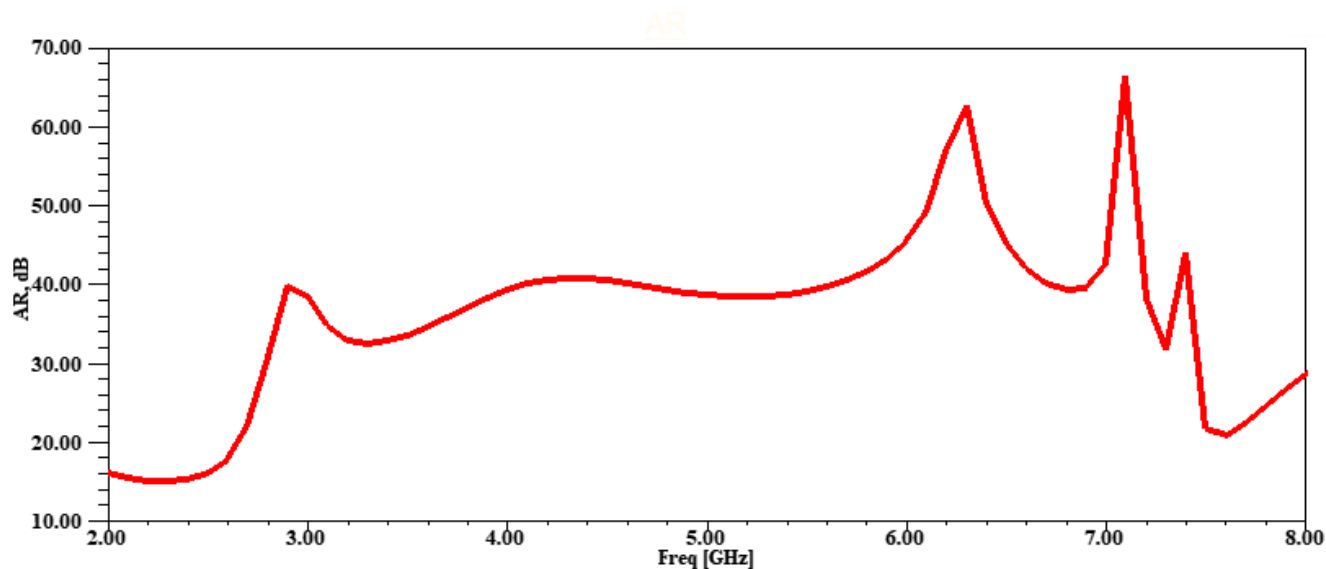


Fig. 7. AR of the LP printed dipole antenna

To validate the results, the CST software is employed for designing and simulating the suggested printed dipole antenna. As depicted in Fig. 8, an excellent agreement between the two software is founded in terms of S_{11} , where the results from both software cover the entire frequency band of the 5G applications.

The 3D-radiation pattern for the linearly polarized dipole antenna has been evaluated and presented in Fig. 9 at various operational frequencies. As depicted in Fig. 9, the antenna has a steady endfire-type radiation pattern over the whole frequency band.

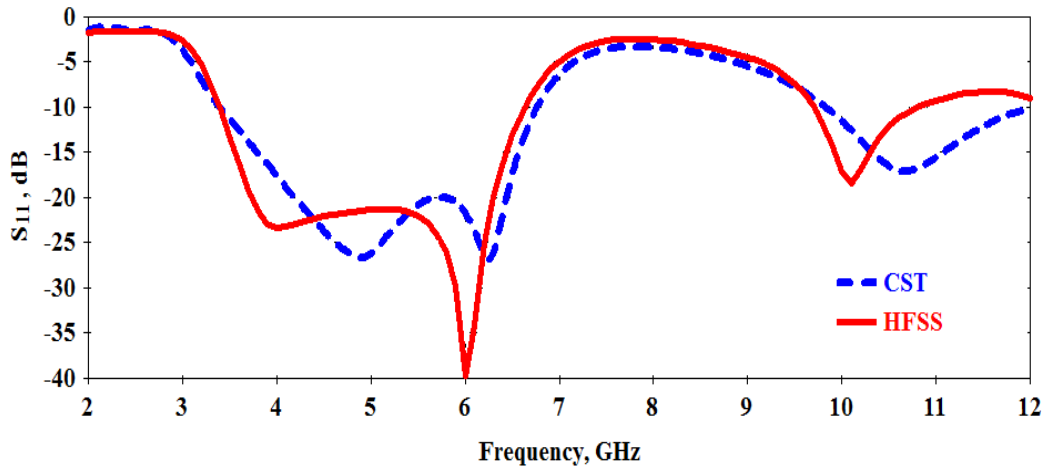


Fig. 8. Comparison of S_{11} for LP printed dipole antenna from both HFSS and CST softwares

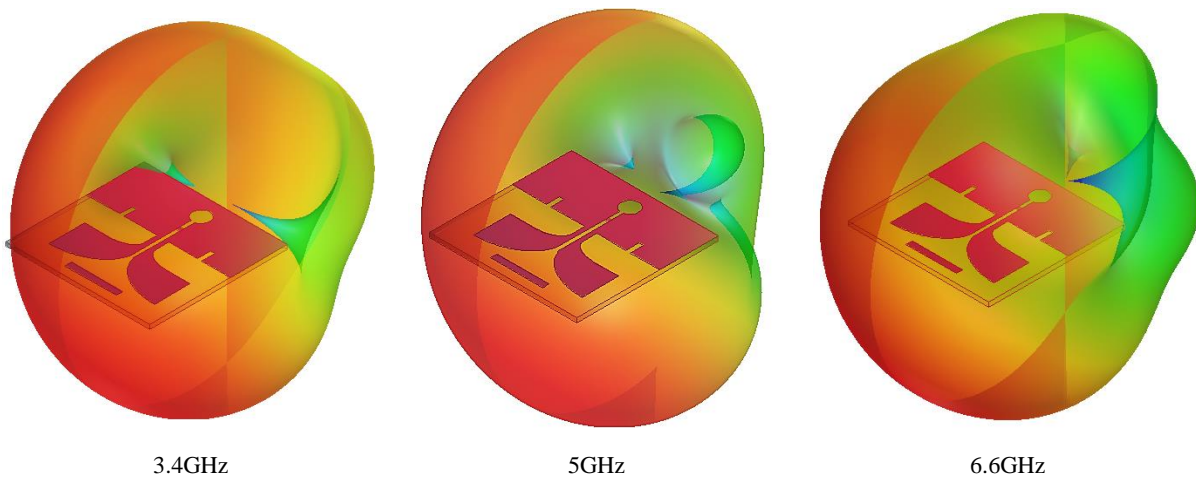


Fig. 9. 3D-radiation pattern of the LP printed dipole antenna

6.2. Circular Polarization Antenna

Fig. 10 depicts the evaluation of the circularly polarized antenna's reflection coefficient (S_{11}). Fig. 10 found that the simulated results show a good IBW of more than 4GHz ranging from 3.9GHz to more than 8GHz at (-10 dB) which covers the whole sub-6 band for 5G.

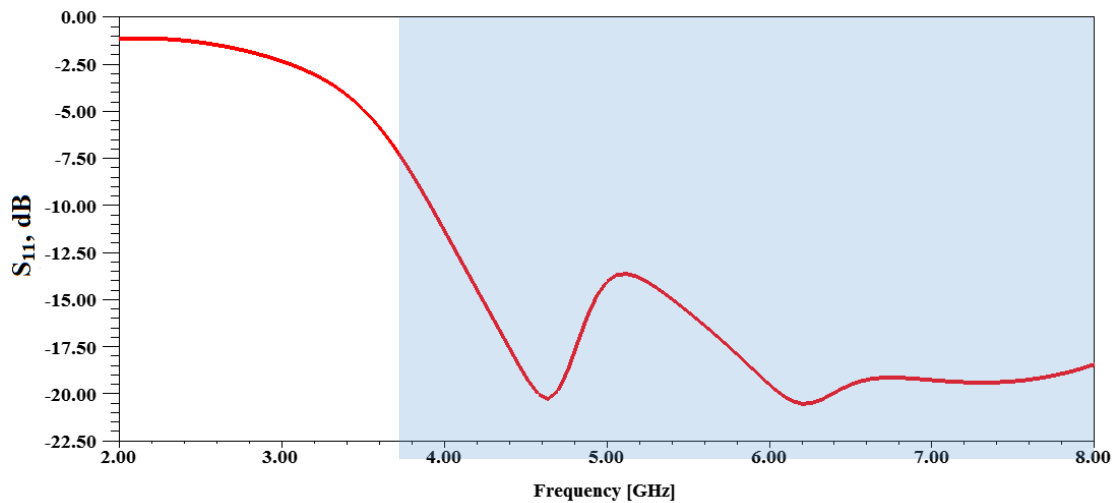


Fig. 10. The reflection coefficient (S_{11}) in dB for the CP CPW-Fed antenna

In Fig. 11, the gain of the circular polarization CPW-Fed printed antenna is displayed. As seen in Fig. 11, the gain varies from 2.8 dB to 4.18 dB over the whole operational frequency band.

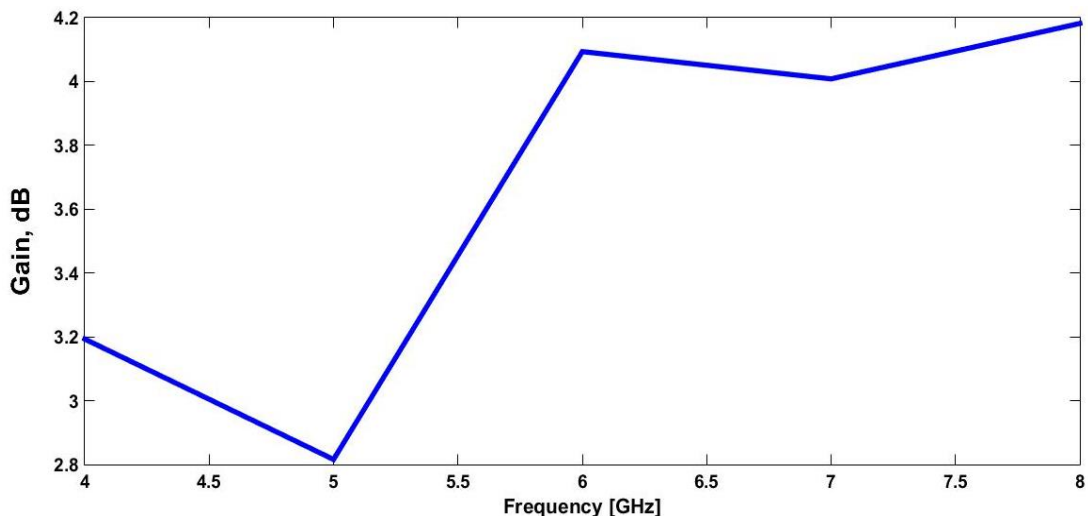


Fig. 11. The gain in dB for the CP CPW-Fed antenna

The axial ratio is evaluated and presented in Fig. 12. As depicted in Fig. 12, the axial ratio varies from 4.2GHz to 7GHz with AR of less than 3 dB so the antenna gives a circular polarization in this band.

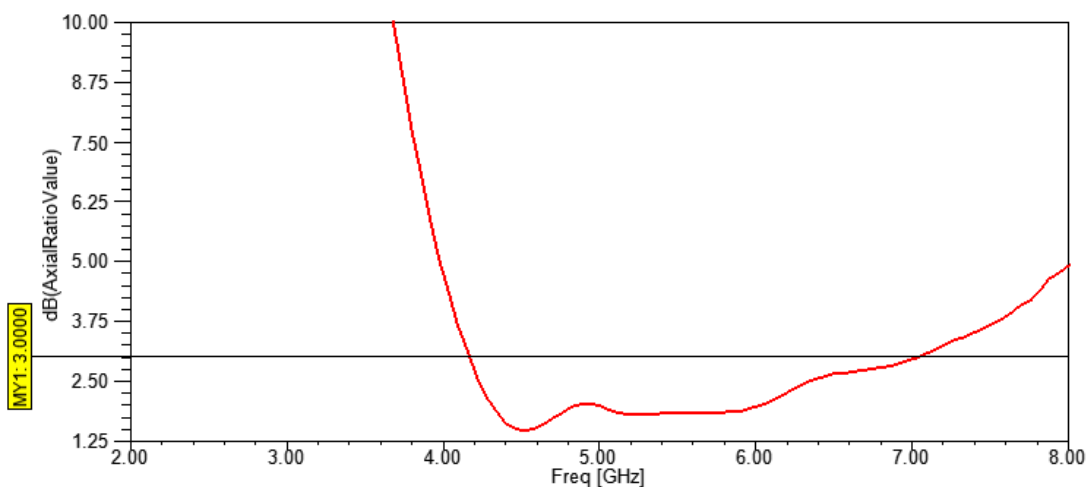


Fig. 12. AR for the CP CPW-Fed antenna

To validate the results, the CST software is employed for designing and simulating the suggested CPW-Fed printed antenna. As depicted in Fig. 13, an excellent agreement between the two software is founded in terms of AR where the results from both software cover the entire frequency band of the 5G applications.

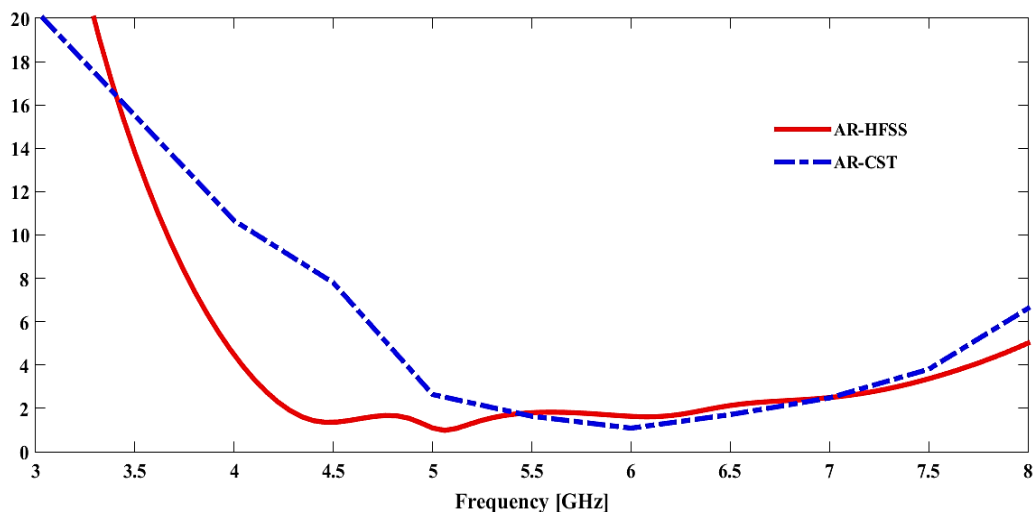


Fig. 13. Comparison of AR for CP CPW-Fed printed antenna from both HFSS and CST softwares

The 3D-radiation pattern of the circular polarization CPW-Fed printed antenna is evaluated and presented in Fig. 14 at different operating frequencies. As seen in Fig. 14, the antenna shows a quasi-omni-directional stable radiation pattern.

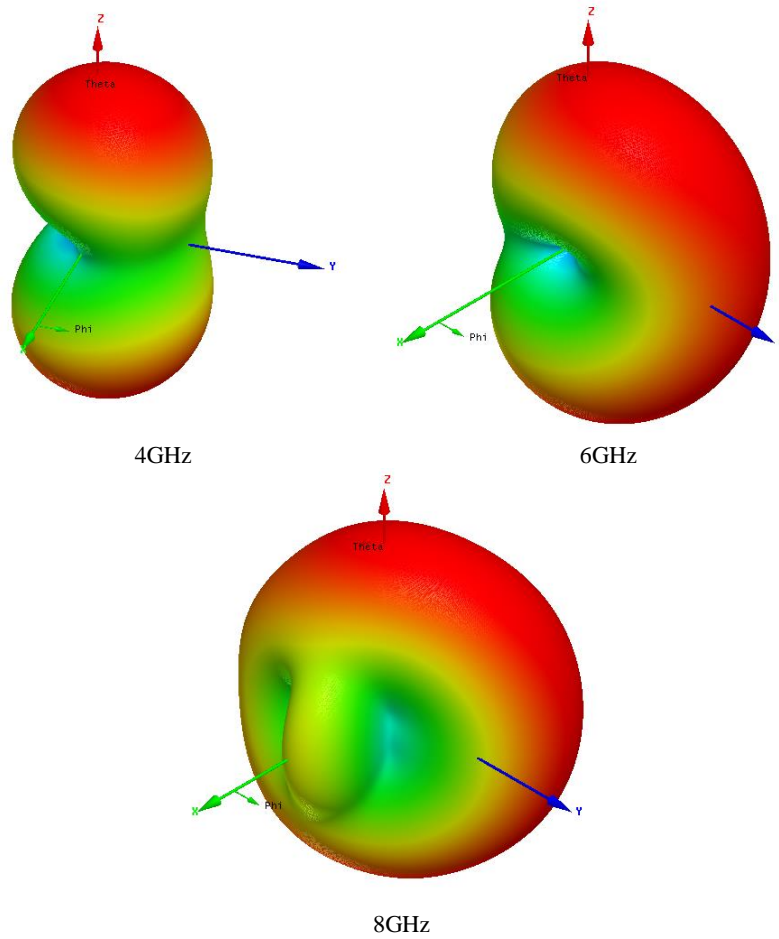


Fig. 14. 3D-radiation-pattern of the CP CPW printed antenna

6.3. Dual Polarizations MIMO Antenna System

The reflection coefficients (S_{ii}) of the suggested MIMO antenna structure in terms of S_{11} , S_{22} , S_{33} , S_{44} , and S_{55} are measured and presented in Fig. 15. The simulation results demonstrate great agreement and give a broad impedance bandwidth. Two impedance bandwidths are found. The first bandwidth is equal to 3.44 GHz, ranging from 3.3GHz to 6.7GHz at (-10 dB). While the second impedance bandwidth is found equal to more than 4.33 GHz, starting from 3.6 GHz to more than 8 GHz at (-10 dB). Both bandwidths cover the whole sub-6GHz frequency bands of the 5 G applications.

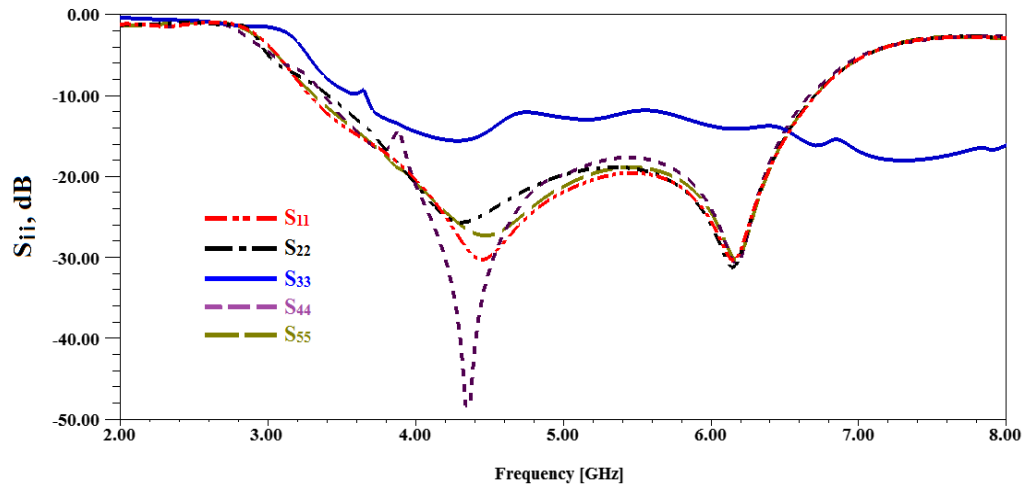


Fig. 15. S_{11} , S_{22} , S_{33} , S_{44} , and S_{55} for the suggested MIMO antenna elements

The transmission coefficients (S_{ij}) for each subsequent pair of MIMO antenna components are measured and shown in Fig. 16 in terms of S_{21} (isolation between the first and second antennas), S_{32} (isolation between the second and third antennas), S_{43} (isolation between the third and fourth antennas), S_{54} (isolation between the fourth and fifth antennas), and S_{15} (isolation between the fifth and first antennas). Because of the very low surface waves inside the substrate of the MIMO antenna, it is seen that excellent isolation exists between MIMO components where all values are greater than the standard value (-20dB) according to [33].

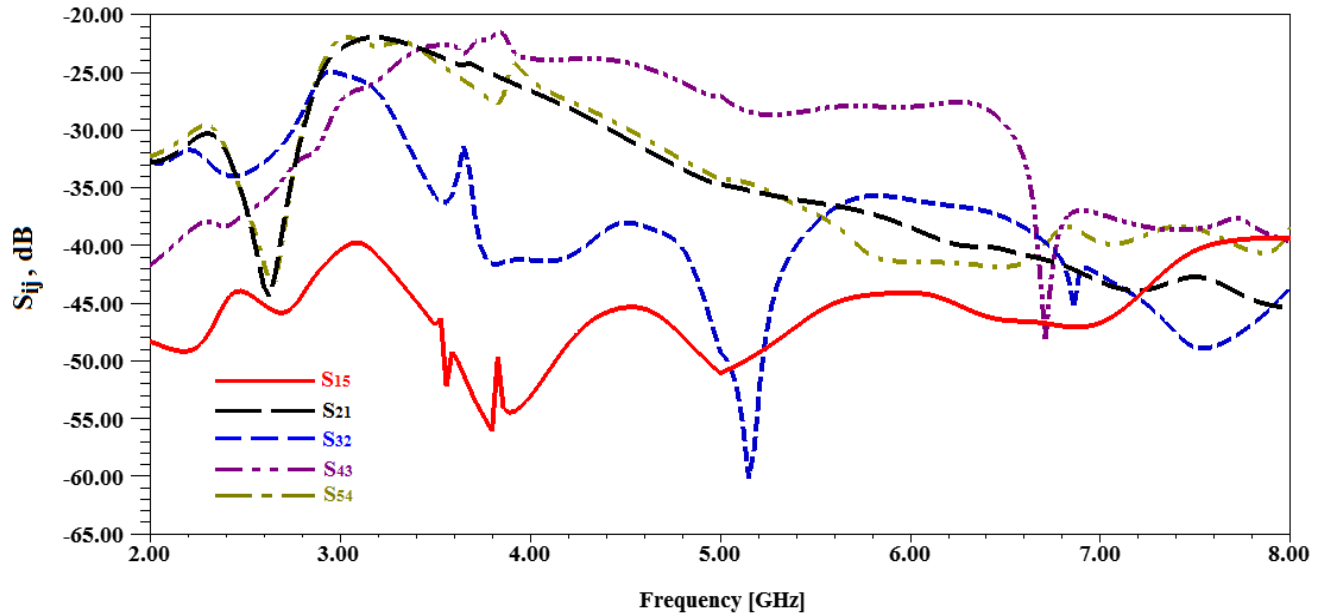


Fig. 16. Mutual coupling (S_{15} , S_{21} , S_{32} , S_{43} , and S_{54}) between the MIMO antenna elements

The 3D radiation-patterns for the MIMO antenna system-based decoupling elements are evaluated for all ports and presented in Fig. 17. Also, Fig. 18 shows the 2D radiation-pattern of the MIMO antenna system based on decoupling elements for all ports in terms of E-Plane and H-Plane. From the measured radiation-patterns of the MIMO antenna system-based decoupling elements, it's found that many types of radiation-patterns can be achieved from such a structure. The CPW-Fed antenna can give a broadside radiation pattern, while the planar dipoles can give omniradiation or directed radiation. This is because you can change the number of planar dipole antennas, so you can make different types of beams.

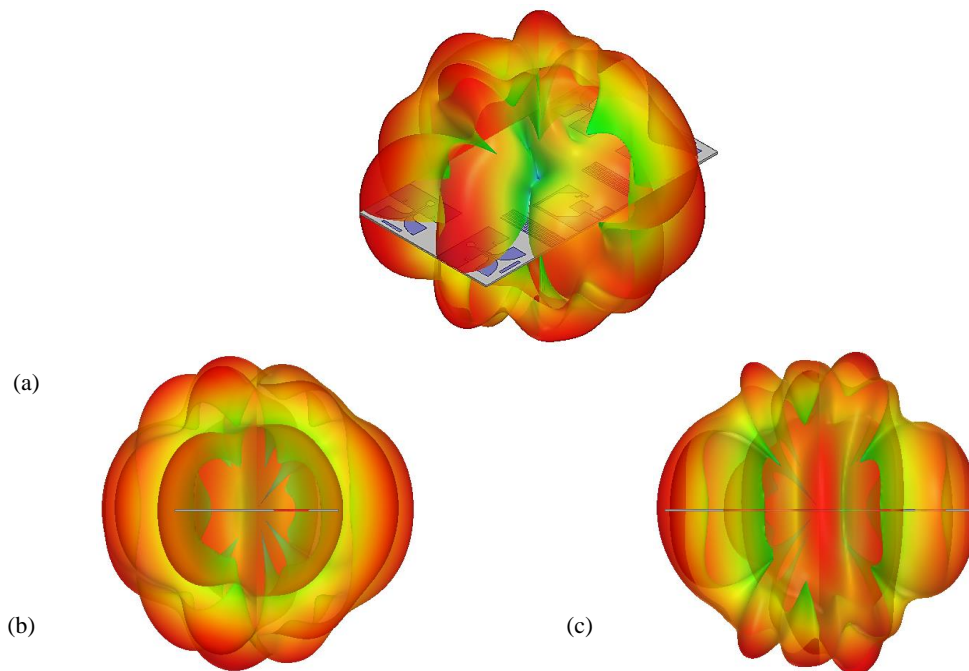


Fig. 17. 3D-radiation patterns of the MIMO antenna system-based decoupling elements for all ports; (a) 3D View, (b) front View, and (c) side View

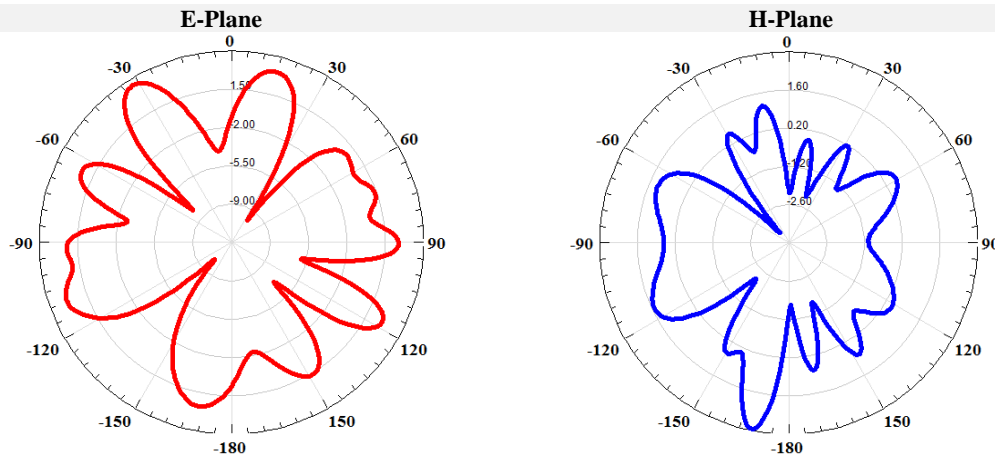


Fig. 18. 2D-radiation pattern of the MIMO Antenna system-based decoupling elements for all ports

7. Conclusion

This study suggests designing a dual polarization MIMO antenna structure based on decoupling elements for sub-6 5G band applications. The MIMO antenna system includes 5 elements with a total size of $150 \times 82.5 \times 1 \text{ mm}^3$. Four elements of the planar dipole antenna and one of CPW-Fed antenna are used to form a MIMO antenna structure and are arranged in some way to produce an Omni-directional radiation-pattern. The planner dipole antenna that has an end-fire radiation is placed in the corners of the substrate and each one is directed toward one of the four directions, while the CPW-Fed printed antenna of the quasi-Omni-directional radiation pattern is placed in the center to produce the Omni-directional radiation pattern. A Meander Line Resonator technique is used and added between the MIMO antenna components to mitigate the mutual coupling between the antennas and to achieve good isolation. Two impedance bandwidths are found. The first one (S_{11} , S_{22} , S_{44} , S_{55}) is equal to 3.44GHz, ranging from 3.3GHz to 6.6GHz at (-10 dB) and gives linear polarization, while the second bandwidth (S_{33}) is equal to 4.33GHz, starting from 3.6GHz to more than 8GHz at (-10 dB) and gives circular polarization from 4.2GHz to 7GHz. The HFSS software environment is utilized for designing and simulating the proposed antennas, and for verifying the results, the CST software is used.

Acknowledgement

When we were working on the prototypes for this study, we received assistance from the Electrical Engineering Technical College-Department of Computer Engineering Techniques at Middle Technical University.

References

- [1] W. Zeng, S. Qi, L. Liu, and Y. Yao, "Research on laser-generated Rayleigh waves with angled surface crack by finite element method," *Optik*, 2019.
- [2] J. Gozavez, "5G Worldwide Developments [Mobile Radio]," in *IEEE Vehicular Technology Magazine*, ed. 2017.
- [3] L. Ge and K. M. Luk, "A wideband magneto-electric dipole antenna," *IEEE Transactions on Antennas and Propagation*, 2012.
- [4] W. X. Liu, Y. Z. Yin, W. L. Xu, and S. L. Zuo, "Compact open-slot antenna with bandwidth enhancement," *IEEE Antennas and Wireless Propagation Letters*, 2011.
- [5] H. T. Hsu, F. Y. Kuo, P. H. J. M. Lu, and O. T. Letters, "Design of WiFi/WiMAX dual-band E-shaped patch antennas through cavity model approach," vol. 52, no. 2, pp. 471-474, 2010.
- [6] T. Abeesh and M. Jayakumar, "Design and studies on dielectric resonator on-chip antennas for millimeter wave wireless applications," in 2011 - International Conference on Signal Processing, Communication, Computing and Networking Technologies, ICSCCN-2011, ed. 2011.
- [7] T. T. Thai, G. R. DeJean, and M. M. Tentzeris, "Design and development of a novel compact soft-surface structure for the front-to-back ratio improvement and size reduction of a microstrip Yagi Array Antenna," *IEEE Antennas and Wireless Propagation Letters*, 2008.
- [8] S. Wang, Q. Wu, and D. Su, "A novel reversed t-match antenna with compact size and low profile for ultrawideband applications," *IEEE Transactions on Antennas and Propagation*, 2012.
- [9] S. Lim and H. Ling, "Design of a closely spaced, folded Yagi antenna," *IEEE Antennas and Wireless Propagation Letters*, 2006.
- [10] S. Poorgholam-Khanjari, F. B. Zarrabi, and S. Jarchi, "Compact and wide-band Quasi Yagi-Uda antenna based on periodic grating ground and coupling method in terahertz regime," *Optik*, 2020.
- [11] J. Huang and A. C. Densmore, "Microstrip yagi array antenna for mobile satellite vehicle application," *IEEE Transactions on Antennas and Propagation*, 1991.
- [12] S. X. Ta, B. Kim, H. Choo, and I. Park, "Wideband quasi-Yagi antenna fed by microstrip-to-slotline transition," *Microwave and Optical Technology Letters*, 2012.
- [13] R. Bansal, "Antenna theory; analysis and design," *Proceedings of the IEEE*, 2008.
- [14] R. N. Simons and R. Q. Lee, "Coplanar waveguide aperture coupled patch antennas with ground Plane/Substrate of finite extent," *Electronics Letters*, 1992.
- [15] R. N. Simons, R. Q. Lee, and G. R. Lindamood, "New coplanar waveguide/stripline feed network for seven patch hexagonal CP subarray,"

Electronics Letters, 1991.

- [16] R. N. Simons, R. Q. Lee, and T. D. Perl, "New techniques for exciting linearly tapered slot antennas with coplanar waveguide," *Electronics Letters*, 1992.
- [17] R. N. Simons and G. E. Ponchak, "Coax-to-channelised coplanar waveguide in-phase N-way, radial power divider," *Electronics Letters*, 1990.
- [18] K.-L. Wong, "Compact and Broadband Microstrip Antennas," *Compact and Broadband Microstrip Antennas*, 2002.
- [19] Y. X. Guo, K. M. Luk, and K. F. Lee, "L-probe proximity-fed short-circuited patch antennas," *Electronics Letters*, 1999.
- [20] Y. X. Guo, K. M. Luk, K. F. Lee, and R. Chair, "A quarter-wave U-shaped patch antenna with two unequal arms for wideband and dual-frequency operation," *IEEE Transactions on Antennas and Propagation*, 2002.
- [21] T. Huynh and K. F. Lee, "Single-layer single-patch wideband microstrip antenna," *Electronics Letters*, 1995.
- [22] W. Swelam, I. Ehtezazi, G. Z. Rafi, and S. Safavi-Naeini, "Broad-band U-slot rectangular patch antenna on a microwave substrate using a novel feeding technique," in *IEEE Antennas and Propagation Society, AP-S International Symposium (Digest)*, ed, 2005.
- [23] K. L. Wong and W. H. Hsu, "Broadband triangular microstrip antenna with U-shaped slot," *Electronics Letters*, 1997.
- [24] R. N. Simons, "Coplanar Waveguide Circuits, Components, and Systems," *Coplanar Waveguide Circuits, Components, and Systems*, 2001.
- [25] R. V. R. Krishna, R. Kumar, and N. Kushwaha, "An UWB dual polarized microstrip fed L-shape slot antenna," *International Journal of Microwave and Wireless Technologies*, 2016.
- [26] Y. Kabalci, "5G Mobile Communication Systems: Fundamentals, Challenges, and Key Technologies," ed, 2019.
- [27] J. Rodriguez, "Fundamentals of 5G Mobile Networks," *Fundamentals of 5G Mobile Networks*, 2015.
- [28] C. H. Wu, C. L. Chiu, and T. G. Ma, "Very Compact Fully Lumped Decoupling Network for a Coupled Two-Element Array," *IEEE Antennas and Wireless Propagation Letters*, 2016.
- [29] S. Gupta, Z. Briqech, A. R. Sebak, and T. Ahmed Denidni, "Mutual-Coupling Reduction Using Metasurface Corrugations for 28 GHz MIMO Applications," *IEEE Antennas and Wireless Propagation Letters*, 2017.
- [30] Y. Li, C. Y. D. Sim, Y. Luo, and G. Yang, "High-Isolation 3.5 GHz Eight-Antenna MIMO Array Using Balanced Open-Slot Antenna Element for 5G Smartphones," *IEEE Transactions on Antennas and Propagation*, 2019.
- [31] A. Dadgarpour, B. Zarghooni, B. S. Virdee, T. A. Denidni, and A. A. Kishk, "Mutual Coupling Reduction in Dielectric Resonator Antennas Using Metasurface Shield for 60-GHz MIMO Systems," *IEEE Antennas and Wireless Propagation Letters*, 2017.
- [32] K. L. Wong and J. Y. Lu, "3.6-GHz 10-antenna array for mimo operation in the smartphone," *Microwave and Optical Technology Letters*, 2015.
- [33] R. S. Parbat, A. R. Tambe, M. B. Kadu, and R. P. Labade, "Dual polarized triple band 4×4 MIMO antenna with novel mutual coupling reduction approach," in *2015 IEEE Bombay Section Symposium: Frontiers of Technology: Fuelling Prosperity of Planet and People*, IBSS 2015, ed, 2016.
- [34] Y. Sharma, D. Sarkar, K. Saurav, and K. V. Srivastava, "Three-Element MIMO Antenna System with Pattern and Polarization Diversity for WLAN Applications," *IEEE Antennas and Wireless Propagation Letters*, 2017.
- [35] N. M. K. Al-Ani, O. A. S. Al-Ani, M. F. Mosleh, and R. A. Abd-Alhameed, "A Design of MIMO System Based on Y-Shaped with QSCS for UWB Applications," *International Journal of Information Technology and Computer Science*, 2020.
- [36] R. K. Jaiswal, K. Kumari, and K. V. Srivastava, "Circularly and linearly polarized MIMO antenna system with pattern and polarization diversity," in *2019 IEEE Indian Conference on Antennas and Propagation, InCAP 2019*, ed, 2019.
- [37] M. Abdullah et al., "Future Smartphone: MIMO Antenna System for 5G Mobile Terminals," *IEEE Access*, 2021.
- [38] A. S. Abdullah, S. A. Hashem, W. S. Al-Dayyeni, M. F. Mosleh, and I. Hassoun, "Four-Port Wideband Circular Polarized MIMO Antenna for Sub-6 GHz Band," in *Lecture Notes in Networks and Systems*, ed, 2022.
- [39] R. Shao, X. Chen, J. Wang, and X. J. E. Wang, "Design and Analysis of an Eight-Port Dual-Polarized High-Efficiency Shared-Radiator MIMO Antenna for 5G Mobile Devices," vol. 11, no. 10, p. 1628, 2022.
- [40] S. Saxena, B. K. Kanaujia, S. Dwari, S. Kumar, H. C. Choi, and K. W. Kim, "Planar Four-Port Dual Circularly-Polarized MIMO Antenna for Sub-6 GHz Band," *IEEE Access*, 2020.